中國機械工程學刊第四十二卷第六期第 571~580 頁(民國一百一十年)
Journal of the Chinese Society of Mechanical Engineers, Vol.42, No.6, pp. 571~580 (2021)

Computer-Aided Sequence Planning for Bending Operations of 3D Sheet Metals with Many Bends in Various Directions

Alan C. Lin* and Chao-Fan Chen**

Keywords: CAD, Sheet metal working.

ABSTRACT

The most complex step in sheet metal production is the bending process, and the planning of a bending sequence directly impacts the feasibility of sheet metal processing. This paper proposes a set of principles to be followed for the planning of bending sequences. It first uses the rule “the more bending lines, the better” to select an appropriate datum plane out of all the possible bending planes of a 3D sheet metal. Based on the selected datum plane, the rule “the smaller angle between bending lines, the better” is applied to divide the sheet metal into a number of bend segments. In the second step, six bending patterns are defined based on the geometric characteristics of various bending operations. Each of the bend segments determined in the first step is then compared with the six bending patterns to obtain a bending sequence for each bend segment. Lastly, the order of the bend segments is arranged by following the principle “minimum-height, first-processed” to obtain the final bending sequence for the entire sheet metal.

INTRODUCTION

Bending is one of the most important aspects in manufacturing processes for sheet metals. However, a sheet metal part with many bends may very well lead to a computational explosion due to the limitless possible combinations generated by various bending sequences. When planning a bending sequence, the main priority is to consider its feasibility, *i.e.*, how to avoid interference between part features, between punches and the part, and between the part and the press machine. Since the aforementioned operation is a multi-faceted thought process, the planning of a bending sequence is a difficult and complex selection process (Duflou et al. 2005). Additionally, although each bending process is only an operation of a punch to the local area of sheet metal, the contour of the entire piece of sheet metal changes as the bending processes proceed, *i.e.*, the sheet metal’s contour has a significant impact on sequence planning for bending operations.

In the past, the task of planning bending operations was performed by process planning engineers, who relied on personal experience or referenced data left by predecessors. Their approach was to perform repeated trials and verifications on every possible bending sequence, then eliminate those unfeasible bending sequences, thus finding the applicable bending sequences. This laborious planning method may be applicable for simple bending projects; however, if the sheet metal part has numerous bends or if the form of the part is unique, then it will be beyond an engineer’s ability to handle. Even if computers are used to assist in sequence planning, it is very easy to encounter a computational explosion.

While the sheet metal’s contour is composed of many geometric features, the impact of various geometric features on the bending sequence can be utilized for planning the bending sequence (Aomura and Koguchi 2002; Kannan and Shunmugam 2009-1 & 2009-2; Raj Prasanth and Shunmugam 2018). If the sheet metal has no definitive geometric model, then it is difficult to plan the bending sequence with geometric features. In this situation, the resulting restrictions for the bending sequence must then be hand-coded, which leads one to question the reliability of the generated bending sequence. For this, one can define domain-specific expert modules between the sheet metal, punches, and press machines, use predefined constraint modules, and satisfy geometric constraints to solve this complex bending problem (Márkus et al. 2002). In addition, one can find feasible bending sequences via punch-selection restrictions and verification of the interference between punches and the sheet metal’s contour (Rico et al. 2003;

Paper Received December 2014. Revised November, 2015, Accepted December, 2015, Author for Correspondence: Alan C. Lin.

* *Professor, Department of Mechanical Engineering, National Taiwan University of Science and Technology, Taipei, Taiwan 106, ROC.*

** *Ph.D. Student, Graduate Institute of Automation and Control, National Taiwan University of Science and Technology, Taipei, Taiwan 106, ROC.*

Cattrysse et al. 2005). If the sheet metal has many bends, geometric constraints and branch-and-bound techniques can be used to reduce the computation time required for the determination of bending sequences (De Vin et al. 2010; Duflou et al. 2010; Faraz et al. 2017).

Furthermore, a virtual node can be used to define each bending process. Steps that can be excluded from consideration of the bending sequence may be identified through the relationship between nodes. Thus, unnecessary computation may be eliminated and bending sequences can be obtained (Gupta 1999). There are also scholars using fuzzy logic to plan bending sequences. They define weights for different rules, including a compound-bends rule, a parallel-bends rule, a shape-determining bend rule, a single-face rule, and a combined rotation rule, then use a fuzzy matrix to perform the calculations required to obtain the best bending sequences (Kim et al. 2002; Kim et al. 2006; Farsi and Arezoo 2009; Abedini et al. 2010). There are also techniques that adopt genetic algorithms, which consider corresponding punches in the bending process in order to obtain the best bending sequences (Thanapandi et al. 2001; Thanapandi et al. 2002; Kannan and Shunmugam 2008; Kontolatis and Vosniakos 2012).

In other cases, to increase the performance of sheet metal production, progressive dies are used to handle notching, punching, bending, and forming processes (Tor et al. 2005-1 & 2005-2). Generally speaking, if the total number of required punches is not high, a superimposition scheme can be used to rapidly produce the notching and bending features to be utilized for planning the sequences of operations of the progressive die. Then, from many possible sequences, a superior and applicable sequence can be identified. However, when the number of punches becomes large, using the superimposition scheme will create a computational explosion problem in itself that needs to be solved. To avoid this problem and to rapidly obtain a feasible solution for sequence planning, one can make a comprehensive examination from the perspectives of strip preparation, punch layout, and layout evaluation, to determine appropriate sequences for the progressive die (Lin and Sheu 2012-1 & 2012-2).

The abovementioned researches concerning sequence planning for bending operations are specifically designed for 2D sheet metals that have less than the average number of bends or that require fewer punches, dies, or bending features. These methods will not be applicable to a 3D sheet metal that contains many bends, due to the numerous interference checks that must be performed for each possible bend on the physical sheet metal. For example, take a sheet metal part that has 11 bends, as shown in Figure 1. There are 39,916,800 (11!) possible bending sequences, which may result in a computational explosion for interference checking.

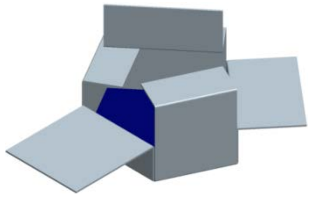

Fig. 1. A 3D sheet metal part containing 11 bends.

To resolve this issue, this research proposes a three-phase bending planning procedure. First, the sheet metal is divided into various bend segments based on a datum plane for bending operations. Then, each bend segment is compared with the six bending patterns to obtain a bending-pattern combination. Lastly, bending sequences for each bend segment are determined to obtain the final bending sequence. Figure 2 shows a flowchart of the proposed method of sequence planning for bending operations. The following sections will explain the three phases of the method in detail, and these explanations will be supplemented by examples.

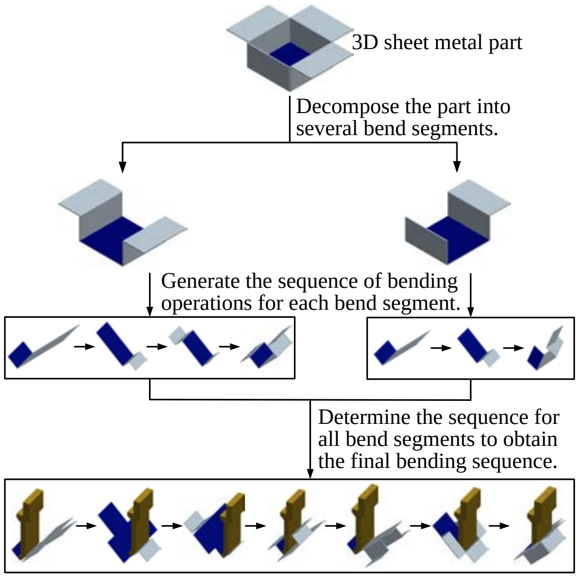

Fig. 2. Flowchart for sequence planning of bending operations for a 3D sheet metal part.

DECOMPOSING A SHEET METAL PART INTO SEVERAL BEND SEGMENTS

The data source for planning a sequence of bending operations is the 3D geometric model of a sheet metal part. From the geometric model, the plane that contains the most bending lines is first chosen as the datum plane for bending operations. For example, in Figure 3, the sheet metal part is composed of twelve bending planes, s_1~s_{12}, and eleven bending lines, b_1~b_{11}. Bending plane s_4 comprises 5 bending lines: b_3, b_4, b_7, b_8, and b_{11}, which makes it the plane that has the most bending lines and, therefore, s_4 is selected as the datum plane for bending operations.

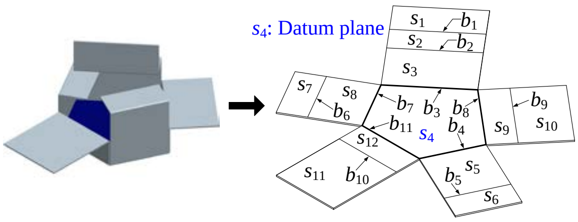

Fig. 3. Illustration of datum plane of bending operations.

Once the datum plane is determined, the angles between every pair of bending lines on the datum plane are calculated. Starting from the minimum angle, adjacent bending planes for each of the two corresponding bending lines are connected to form a bend segment, until the entire set of bending lines are searched through. Each bend segment thus comprises the datum plane, the bending lines of the datum plane, and their connected bending planes. Each bend segment can be regarded as an independent 2.5D sheet metal part.

Using the sheet metal part in Figure 3 as an example, the steps for the generation of bend segments are as follows:

(1) Calculate the angles between bending lines: On datum plane s_4, there are 5 bending lines: b_3, b_8, b_4, b_{11}, and b_7. By calculating the angle between every pair of bending lines, one can obtain the following results (see Figure 4): 100° between b_3 and b_7, 40° between b_3 and b_{11}, 25° between b_3 and b_4, 100° between b_3 and b_8, 120° between b_7 and b_{11}, 55° between b_7 and b_4, 20° between b_7 and b_8, 115° between b_{11} and b_4, 40° between b_{11} and b_8, and 105° between b_4 and b_8.

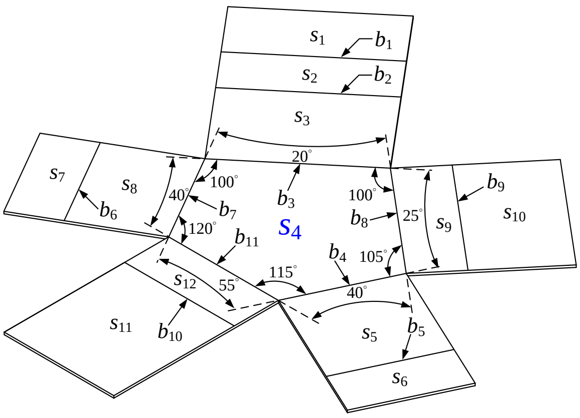

Fig. 4. Angles between bending lines.

(2) Decompose the 3D sheet metal part into several 2.5D bend segments: Of all the above angles, the angle between b_7 and b_8 is the smallest (20°); thus, the bending planes extending from b_7 and b_8 form bend segment #1. That is, segment #1 is composed of datum plane s_4, bending planes s_7~s_{10}, and bending lines b_6~b_9, as shown in Figure 5(*a*). The angle of 25° between b_3 and b_4 is the second smallest; thus, bend segment #2 can be formed and is composed of datum plane s_4, bending planes s_1, s_2, s_3, s_5, and s_6, and bending lines b_1~b_5, as shown in Figure 5(*b*). After bend segments #1 and #2 are divided, the only bending line left on the datum plane is b_{11}; thus, bend segment #3 is composed of datum plane s_4, bending planes s_{11} and s_{12}, and bending lines b_{10} and b_{11}, as shown in Figure 5(*c*).

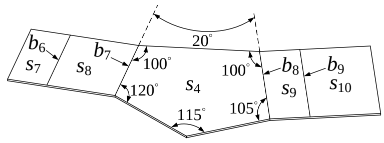

(*a*) Bend segment #1

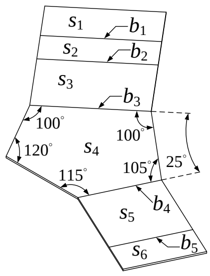

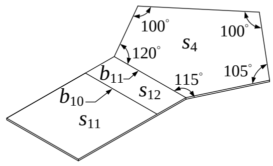

(*b*) Bend segment #2 (*c*) Bend segment #3

Fig. 5. Three bend segments.

GENERATING THE SEQUENCE OF BENDING OPERATIONS FOR EACH OF THE BEND SEGMENTS

To perform sequence planning for a bend segment, which is a 2.5D sheet metal part, this study first defines six basic bending patterns as shown in Table 1: *L*-type, *Z*-type, *U*-type, *C*-type, *P*-type, and *Ω*-type (Lin and Chen 2014). Each bending pattern is assigned a set of codes and has its own bending sequence. In a bend segment, the sheet metal planes and their connection patterns are represented by codes. These codes are compared with the codes of the six bending patterns in order to decompose a bend segment into various bending patterns. The procedure is as follows:

(1) Determine if any of the codes in the bend segment match the codes of the *Ω*-type pattern. If so, then set aside the portion of bend-segment codes that match the codes of the *Ω*-type pattern. Continue with the remaining codes to determine if there are more *Ω*-type pattern codes. If yes, then again set aside the portion of codes that match *Ω*-type pattern codes. Repeat this process until all the codes are sorted.

(2) Continue with the remaining codes to determine if they match the codes of the *P*-type pattern. If so, then set aside the portion of bend-segment codes that match the codes of the *P*-type pattern.

Table 1. Illustration of six bending patterns and corresponding bending sequences.

Type	Example	Symbol	Bending sequence
L type	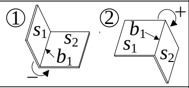	① s_1-s_2 ② s_1+s_2	
Z type	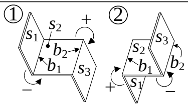	① $s_1-s_2+s_3$ ② $s_1+s_2-s_3$	① $b_1 \rightarrow b_2$ ② $b_1 \rightarrow b_2$
U type	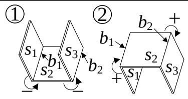	① $s_1-s_2-s_3$ ② $s_1+s_2+s_3$	① $b_1 \rightarrow b_2$ ② $b_1 \rightarrow b_2$
C Type	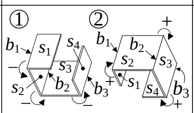	① $s_1-s_2-s_3-s_4$ ② $s_1+s_2+s_3+s_4$	① $b_1 \rightarrow b_3 \rightarrow b_2$ ② $b_1 \rightarrow b_3 \rightarrow b_2$
P Type	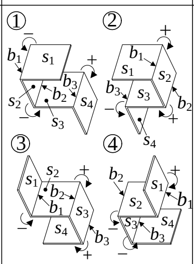	① $s_1-s_2-s_3+s_4$ ② $s_1+s_2+s_3-s_4$ ③ $s_1-s_2+s_3+s_4$ ④ $s_1+s_2-s_3-s_4$	① $b_3 \rightarrow b_2 \rightarrow b_1$ ② $b_3 \rightarrow b_2 \rightarrow b_1$ ③ $b_1 \rightarrow b_2 \rightarrow b_3$ ④ $b_1 \rightarrow b_2 \rightarrow b_3$
Ω Type	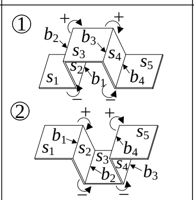	① $s_1-s_2+s_3+s_4-s_5$ ② $s_1+s_2-s_3-s_4+s_5$	① $b_1 \rightarrow b_2 \rightarrow b_4 \rightarrow b_3$ ② $b_1 \rightarrow b_2 \rightarrow b_4 \rightarrow b_3$

Continue with the remaining codes to determine if there are more *P*-type pattern codes. If yes, then again set aside the portion of codes that match *P*-type pattern codes. Repeat this process until all the codes are sorted.

(3) Continue on as above to determine if the remaining codes match *C*-type, *Z*-type, *U*-type, or *L*-type pattern codes, individually. If yes, then set aside these codes. Repeat the process until all the remaining codes are sorted.

Follow the above process to decompose every bend segment into various bending patterns, and then sort these bending patterns following the sequence: *Ω*-type → *P*-type → *C*-type → *Z*-type → *U*-type → *L*-type. That is, start with *Ω*-type bending, followed by *P*-type bending, and so on, until it reaches the final *L*-type bending. Thus, the bending sequence for the bend segment is obtained. Using the sheet metal part in Figure 3 as an example, the codes for bend segment #1 are $s_7-s_8-s_4-s_9+s_{10}$ (see Figure 6(*a*)), and its connection codes are − − − +; the codes for bend segment #2 are $s_1+s_2-s_3-s_4-s_5-s_6$ (see Figure 6(*b*)), and its connection codes are + − − − −; the codes for bend segment #3 are $s_{11}+s_{12}-s_4$ (see Figure 6(*c*)), and its connection codes are + −. The steps used to generate the bending sequences for the three bend segments are illustrated as follows:

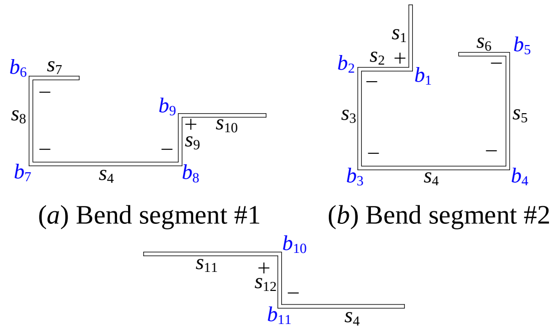

(*a*) Bend segment #1 (*b*) Bend segment #2

(*c*) Bend segment #3

Fig. 6. Formulation of bending codes for the 3 bend segments.

(1) Bend segment #1

The codes for bend segment #1 are $s_7-s_8-s_4-s_9+s_{10}$. The following steps are used to decompose the segment into various bending patterns (see Figure 7):

1 2 3 4: − − − + ≠ Ω-type − + + − ; ≠ + − − + → 1 2 3: − − − ≠ *P*-type − − + ; ≠ + + − ; ≠ − + + ; ≠ + − −

→ 2 3 4: − − + = *P*-type − − + → 1: − = *L*-type −

Results: 1 2 3 4 − − − + can be decomposed into *P*-type 2 3 4 − − + and *L*-type 1 −

Graphical representation:

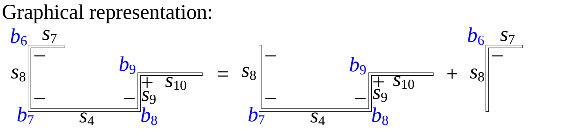

Fig. 7. Code analysis and bending-pattern comparison of bend segment #1.

- The first four codes, − − − +, are taken and compared with the *Ω*-type codes − + + − and + − − + (refer to Table 1 for the codes of each bending pattern). The results show that they do not match.
- Use the first to third codes − − − to compare with the *P*-type codes − − +, + + −, − + +, and + − −. The results show that they do not match.
- Take the second to the fourth codes, − − +, and compare them to the *P*-type codes. The results show that there is a match, thus one *P*-type pattern is obtained. The second to fourth codes are removed from the entire set of codes with the first code, −, remaining.
- Only the *L*-type pattern of all six bending patterns is composed of one code. Therefore, the single remaining code is an *L*-type pattern.

The above analysis shows that bend segment #1 comprises one *P*-type pattern and one *L*-type pattern. As mentioned above, the rule for a bending-pattern sequence is: *Ω*-type → *P*-type → *C*-type → *Z*-type → *U*-type → *L*-type. Therefore, the sequence for bend segment #1 is to perform a *P*-type bending first, and then an *L*-type bending. Furthermore, Figure 7 reveals that the bending lines for bend segment #1 are b_6~b_9, and, from Table 1, it can be found that the sequence for *P*-type bending is $b_9 \rightarrow b_8 \rightarrow b_7$. Thus, the bending sequence for bend segment #1 is: $b_9 \rightarrow b_8 \rightarrow b_7 \rightarrow b_6$. Figure 8 shows the bending process.

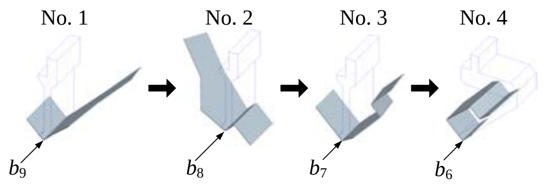

No. 1 ~ No. 3 are *P*-type bends ($b_9 \rightarrow b_8 \rightarrow b_7$).
No. 4 is an *L*-type bend (b_6).

Fig. 8. Bending process of bend segment #1.

(2) Bend segment #2

The codes for bend segment #2 are s_1+s_2−s_3−s_4−s_5−s_6. The following steps are used to decompose the segment into various bending patterns (see Figure 9):

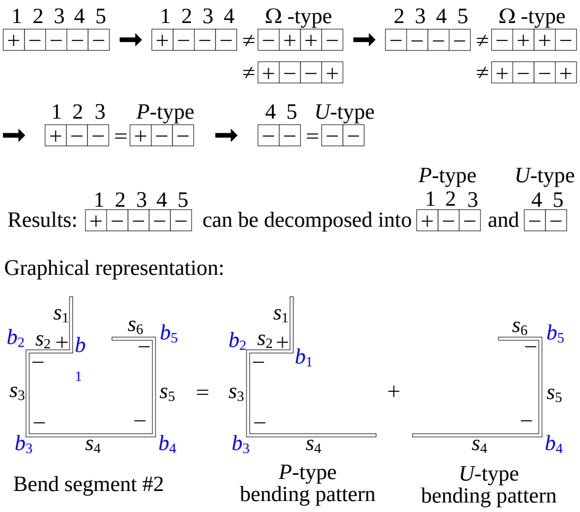

Fig. 9. Code analysis and bending-pattern comparison of bend segment #2.

- Take the first four codes, + − − −, to compare with the *Ω*-type codes − + + − and + − − +. The results show that they do not match.
- Take the next four codes, − − − −, to compare with the *Ω*-type codes − + + − and + − − +. The results show that they do not match.
- Use the first three codes, + − −, to compare with the *P*-type codes − − +, + + −, − + +, and + − −. The results show that there is a match, and thus one *P*-type pattern is obtained. The first three codes are then removed from the entire set of codes, with the fourth and fifth codes, − −, remaining.
- The codes − − are compared with the *U*-type codes − − and + +. There is a match, and thus one *U*-type pattern is obtained.

The above analysis shows that bend segment #2 comprises one *P*-type pattern and one *U*-type pattern. From Figure 9 and Table 1, it can be seen that the sequence for *P*-type bending is $b_1 \rightarrow b_2 \rightarrow b_3$, and the sequence for *U*-type bending is $b_5 \rightarrow b_4$. Also, according to the rule for the bending-pattern sequence: *Ω*-type → *P*-type → *C*-type → *Z*-type → *U*-type → *L*-type, the sequence for bend segment #2 is to perform *P*-type bending first, followed by *U*-type bending. Therefore, the bending sequence for bend segment #2 is: $b_1 \rightarrow b_2 \rightarrow b_3 \rightarrow b_5 \rightarrow b_4$. Figure 10 shows the bending process.

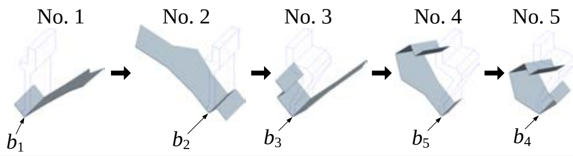

No. 1 ~ No. 3 are *P*-type bends ($b_1 \rightarrow b_2 \rightarrow b_3$).
No. 4 and No. 5 are *U*-type bends ($b_5 \rightarrow b_4$).

Fig. 10. Bending process of bend segment #2.

(3) Bend segment #3

The codes for bend segment #3 are s_{11}+s_{12}−s_4. The following steps decompose the segment into various bending patterns (refer to Figure 11):

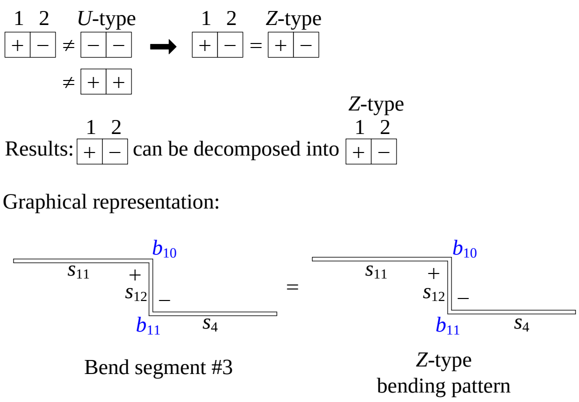

Fig. 11. Code analysis and bending-pattern comparison of bend segment #3.

- There are only two codes in bend segment #3, excluding *Ω*-type, *P*-type, or *C*-type bending patterns, which require more than two codes. Therefore, the first and the second codes, + −, are compared directly to the *U*-type codes − − and + +. The results show that they do not match.
- Compare the first and the second codes, + −, to the *Z*-type bending codes − + and + −. The results show that there is a match, and thus one *Z*-type pattern is obtained.
- Bend segment #3 comprises only one *Z*-type pattern; therefore, there is no need for the sorting process for the various segments. The bending sequence is $b_{10} \rightarrow b_{11}$. Figure 12 shows its bending process.

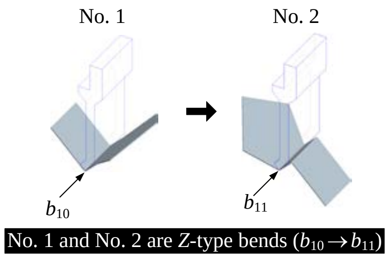

Fig. 12. Bending process of bend segment #3.

DETERMINING THE SEQUENCE FOR BEND SEGMENTS

After all bending patterns of each bend segment have been sorted, one can then proceed to sort all the bend segments to obtain the bending sequence of the entire sheet metal part. A "minimum-height, first-processed" principle is adopted to undertake the sequencing task, where the height is defined as the distance between the bending plane and the datum plane. For example, in Figure 13(a), the height of plane s_7 of bend segment #1 is less than that of plane s_2 of bend segment #2. If plane s_7 is bent first, followed by plane s_2, then there will be no interference (see Figure 13(b)). On the contrary, if plane s_2 is bent first, then plane s_7 will collide with plane s_2 during its bending process (see Figure 13(c)). Expanding from this basic idea, the procedure of sequence planning for bend segments is as follows:

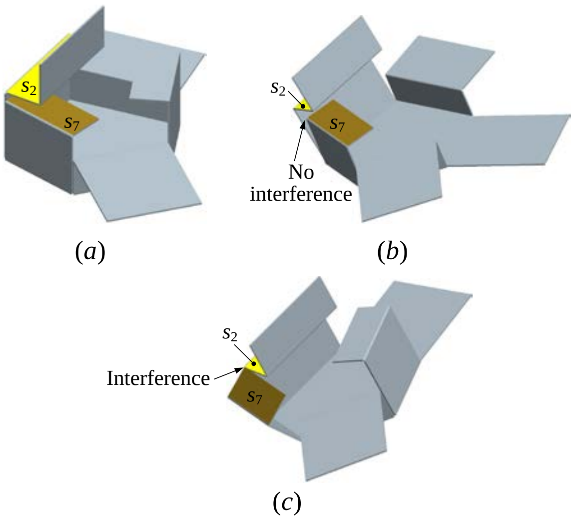

Fig. 13. Illustration of the concept "minimum-height, first-processed".

(1) After setting the datum plane of bending operations as the projection plane, project all bending planes of the sheet metal perpendicularly onto the projection plane to produce projected surfaces.

(2) Determine if the datum plane overlaps any projected surface.

(2.1) If not, then the bending sequence of the bend segments can be arranged arbitrarily without danger of geometric interference.

(2.2) If yes, then determine if the projected surfaces are from the same bend segment.

(2.2.1) If yes, then set the bend segment to be bent last to avoid interference.

(2.2.2) If not, then, for each individual bend segment, determine if it contains any bending planes that are projected onto the datum plane to produce projected surfaces.

(2.2.2.1) If yes, then set the bend segment with the bending plane closest to the datum plane to be bent first, followed by the next closest bend segment. Following this order, the bend segment that is the farthest away is the last to be bent.

(2.2.2.2) If not, then set the bend segment that does not have a projected surface onto the datum plane to be bent first to avoid interference. Then, set the bend segment that has bending planes closest to the datum plane to be bent next. Following this order, the bend segment that is the farthest away is to be bent last.

Using the sheet metal part in Figure 14(a) as an example, the steps of sequence planning for the three bend segments are as follows:

(1) Project bending planes s_1~s_3 and s_5~s_{12} onto datum plane s_4, and obtain projected surfaces p-s_2, p-s_6, p-s_7, p-s_{10}, and p-s_{11}, and projected lines p-s_1, p-s_3, p-s_5, p-s_8, p-s_9, and p-s_{12}, as shown in Figure 14(b).

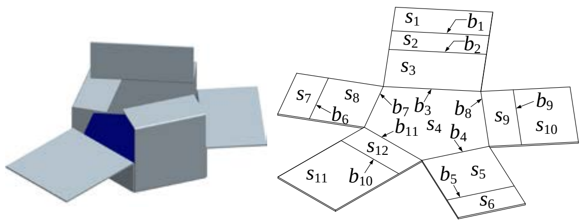

(a) 3D view and flattened view

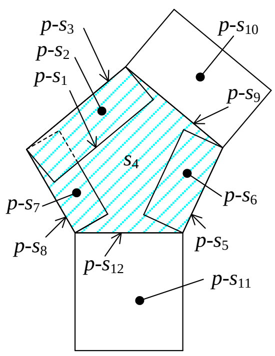

(b) Top view

Fig. 14. Project bending planes onto datum plane.

(2) It can be found that the projected surfaces p-s_2, p-s_6, and p-s_7 all fall inside the datum plane s_4,

which fits condition (2.2) shown above. Among them, p-s_7 is the projection of bending plane s_7 from bend segment #1, and p-s_2 and p-s_6 are projections of s_2 and s_6 from bend segment #2, fitting condition (2.2.2). Bend segment #3 does not have any projected surfaces inside the datum plane.

(3) Calculating the distance between bending planes s_2, s_6, and s_7 and the datum plane, one finds that s_7 has the minimum distance, while s_6 has the maximum, as shown in Figure 15. Thus bend segment #3 is to be bent first (based on condition (2.2.2.1)), followed by bend segment #1, and bend segment #2 will be the last (based on condition (2.2.2.2)).

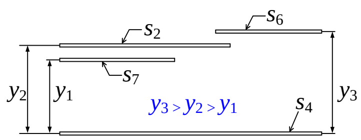

Fig. 15. The distance between bending planes and the datum plane (front view).

Combining the above result with the bending sequences of bend segments #3, #1, and #2 shown in Figures 12, 8, and 10, it is concluded that the bending sequence for the sheet metal part is: $b_{10} \rightarrow b_{11} \rightarrow b_9 \rightarrow b_8 \rightarrow b_7 \rightarrow b_6 \rightarrow b_1 \rightarrow b_2 \rightarrow b_3 \rightarrow b_5 \rightarrow b_4$. The entire bending process for the sheet metal part is illustrated in Figure 16.

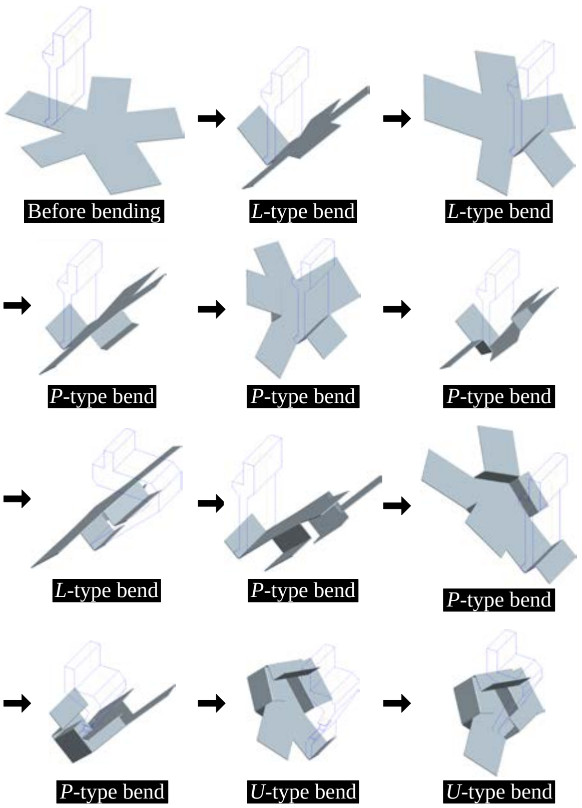

Fig. 16. Bending process for the sheet metal in Figure 14.

SYSTEM IMPLEMENTATION

In addition to proposing methodologies to find appropriate sequences for bending operations of sheet metal parts with multiple bends, this research also uses the commercial software packages Creo and Matlab to implement the algorithms for the proposed methodologies. First of all, Creo is used to create the 3D solid model and the 2D flattened model of a sheet metal part. The application programming interface (or API) subroutines inside Creo are used to retrieve the geometry and topology of the bending planes and bending lines from the 3D and 2D geometric models. The retrieved information is then used as the input for the Matlab program to implement the three modules discussed in the previous sections, that is: (1) decomposing a sheet metal part into several bend segments, (2) generating a sequence of bending operations inside each bend segment, and (3) determining a sequence for bend segments. The output from the Matlab program is a list of bending lines to represent the sequence of bending operations, for instance, b10--b11--b9--b8--b7--b6--b1--b2--b3-- b5--b4 for the process shown in Figure 16. Finally, Creo is used to graphically illustrate the entire bending process.

A number of sheet metal parts are used as testing examples to verify the applicability of the implemented system. One of these examples is shown in Figure 17, which comprises eleven bending planes s_1~s_{11} and ten bending lines b_1~b_{10}. Plane s_4 is comprised of four bending lines b_3, b_4, b_7, and b_8; this is the most bending lines, and, therefore, s_4 is chosen as the datum plane of the bending process. Once the datum plane is determined, the angles between the bending lines of the datum plane are used to divide the sheet metal into several bend segments. The angles between b_3 and b_8, b_8 and b_4, b_4 and b_7, and b_7 and b_3 are all 90°, while the angles between b_3 and b_4, and b_7 and b_8 are all 0° (see Figure 17). Thus, because the angles between b_3 and b_4, and b_7 and b_8 are the smallest, the bending planes connected with b_3 and b_4 are formed as bend segment #1. Its codes are $s_1+s_2-s_3-s_4-s_5-s_6$ (see Figure 18(a)). The bending planes connected with b_7 and b_8 are formed as bend segment #2. Its codes are $s_7+s_8-s_4-s_9+s_{10}+s_{11}$ (see Figure 18(b)).

Once bend segments #1 and #2 are determined, the bending sequences of the two bend segments are generated. The steps are illustrated as follows:

(1) Bending patterns of bend segment #1 and their sequencing.

Use the following steps to decompose bend segment #1 into several bending patterns (refer to Figure 19):

- Take the first to fourth codes, + − − −, of $s_1+s_2-s_3-s_4-s_5-s_6$, and compare them with the codes − + + − and + − − + of the Ω-type pattern. The results show that they do not match.

- Use the first to third codes, + − −, and compare them to the *P*-type codes − − +, + + −, − + +, and + − −. The results show that there is a match, and thus one *P*-type pattern is obtained. The first to third codes are removed from the code list, with the fourth and fifth codes, − −, remaining.
- The remaining two codes indicate that *Ω*-type, *P*-type, and *C*-type bending patterns are excluded in the comparison. Thus, the remaining fourth and fifth codes, − −, are compared to the *U*-type codes, − − and + +. The results show that there is a match, and thus one *U*-type pattern is obtained.

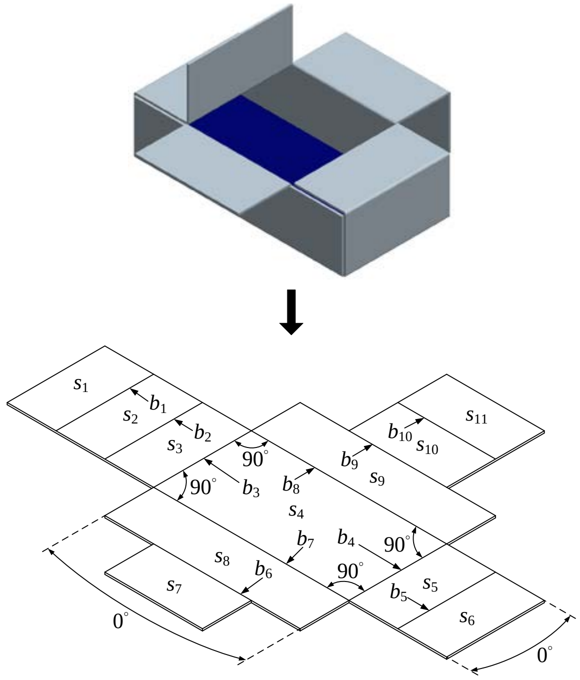

Fig. 17. Datum plane of bending process and angles between bending lines.

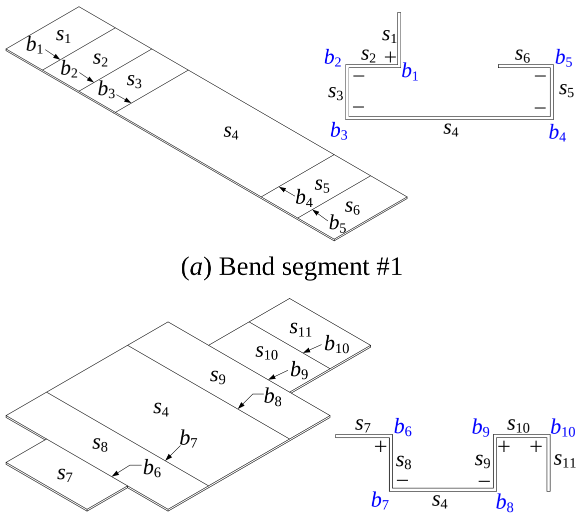

(*a*) Bend segment #1

(*b*) Bend segment #2

Fig. 18. Decomposing the sheet metal into 2 bend segments.

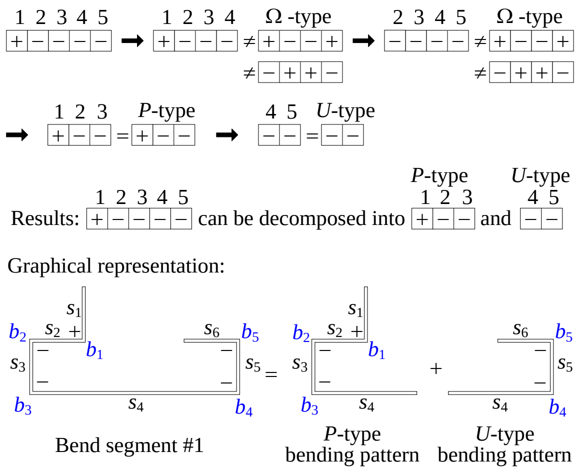

Fig. 19. Two bending patterns of bend segment #1.

Figure 19 illustrates the two bending patterns, *P*-type and *U*-type, that compose bend segment #1. The figure also reveals that the bending lines for the *P*-type bending are b_1~b_3, and for the *U*-type bending are b_4 and b_5. From Table 1, it can be found that the sequence for *P*-type bending is $b_1 \rightarrow b_2 \rightarrow b_3$, and for *U*-type bending it is $b_5 \rightarrow b_4$. Thus, the bending sequence for bend segment #1 is: $b_1 \rightarrow b_2 \rightarrow b_3 \rightarrow b_5 \rightarrow b_4$. Figure 20 shows the bending process.

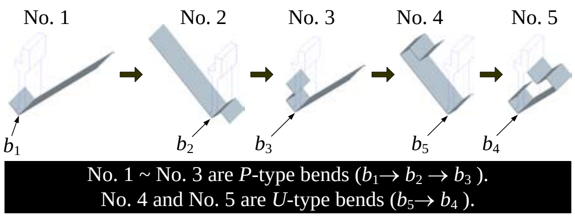

Fig. 20. Bending process of bend segment #1.

(2) Bending patterns of bend segment #2 and their sequencing.

The following steps are used to decompose bend segment #2 into several bending patterns (refer to Figure 21):

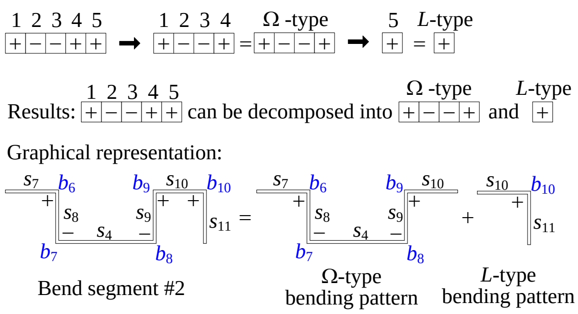

Fig. 21. Two bending patterns of bend segment #2.

- Take the first to fourth codes, + − − +, out of the bending codes $s_7+s_8-s_4-s_9+s_{10}+s_{11}$ of this segment, and compare them to the bending codes − + + − and + − − + of the *Ω*-type patterns. The results show that there is a match. Thus, one *Ω*-type pattern is obtained, and the first to fourth codes are removed from the code list with the fifth code,

−, remaining.

- Of all the bending patterns, only the *L*-type is composed of one code. Therefore the remaining fifth code is *L*-type.

Figure 21 illustrates the two bending patterns, *Ω*-type and *L*-type, that compose bend segment #2. By referencing the sequencing rule for the bending patterns, the *Ω*-type is processed prior to the *L*-type. Thus, the bending sequence of bend segment #2 is $b_6 \rightarrow b_7 \rightarrow b_9 \rightarrow b_8 \rightarrow b_{10}$. Figure 22 shows the bending process.

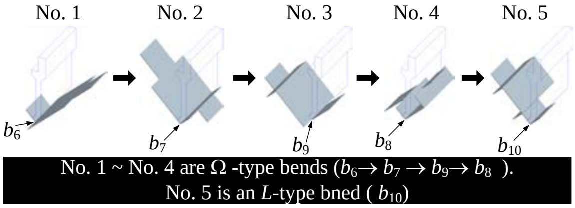

Fig. 22. Bending process of bend segment #2.

After the sequencing of the bending patterns of bend segments #1 and #2 is completed, we determine the sequences of these two bend segments. The steps are as follows:

(1) Project bending planes s_1~s_3 and s_5~s_{11} onto datum plane s_4, and obtain the projected surfaces p-s_2, p-s_6, p-s_7, and p-s_{10}; and projected lines p-s_1, p-s_3, p-s_5, p-s_8, p-s_9, and p-s_{11}, as shown in Figure 23.

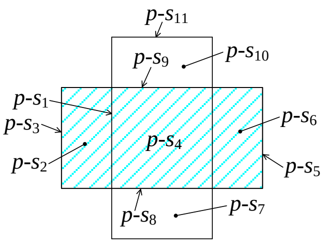

Fig. 23. Project bending planes onto the datum plane.

(2) From the projections, one can see that the projected surfaces p-s_2 and p-s_6 of bending planes s_2 and s_6 are located inside the datum plane s_4, and that both bending planes s_2 and s_6 belong to bend segment #1. Meanwhile, in bend segment #2, there are no projected surfaces in the datum plane. Based on the principles of sequencing bend segments, the following can be concluded: bend segment #2 is to be bent first, followed by bend segment #1. That is, the bending sequence of the sheet metal is: $b_6 \rightarrow b_7 \rightarrow b_9 \rightarrow b_8 \rightarrow b_{10} \rightarrow b_1 \rightarrow b_2 \rightarrow b_3 \rightarrow b_5 \rightarrow b_4$. Figure 24 shows the bending process.

CONCLUSIONS

The planning of bending sequences of sheet metal parts is a complex process. This research proposed a set of principles that can be followed when planning the bending sequence of a 3D sheet metal with many bends in various bending directions. This involved first using the datum plane of bending operations as a base for dividing the 3D sheet metal into various 2.5D bend segments. Next, it used six predefined bending patterns and the sheet metal contours of each bend segment to perform comparisons and decompositions. Then it sorted the bending patterns obtained from the decomposition process and defined priorities for bending. Finally, it used the principle "minimum-height, first-processed" to sort the bend segments, in order to obtain the bending sequence for the entire sheet metal part. The proposed method not only significantly shortens the efforts required for planning a sheet metal's bending sequence, but also establishes a set of simple and systematic planning models for bending sequences.

REFERENCES

Abedini, V., Shakeri, M. and Arezoo, B., "Computer-Aided of bending progressive die design using fuzzy set theory," *CIRP Annals*, Vol. 66, pp. 657-671 (2010).

Aomura S. and Koguchi, A., "Optimized bending sequences of sheet metal bending by robot," *Robotics and Computer-Integrated Manufacturing*, 18 (2002) 29-39.

Cattrysse, D., Collin, P., Duflou, J., Nguyen, H.M.T. and Oudheusden, D.V., "The integration of CAPP and production planning for bent sheet metals", *Advanced Materials Research*, Vols. 6-8, pp. 263-270 (2005).

De Vin, L.J., De Vries, J. and Streppel, T. "Process planning for small batch manufacturing of sheet metals," *International Journal of Production Research*, Vol. 38, No. 17, pp. 4273-4283 (2010).

Duflou, J., Van Oudheusden, D., Kruth, J.-P. and D. Cattrysse, "Methods for the sequencing of sheet metal bending operations," *International Journal of Production Research*, Vol. 37, No. 14, pp. 3185-3202 (2010).

Duflou, J., Váncza, J. and Aerens, R., "Computer aided process planning for sheet metal bending: A state of the art," *Computers in Industry*, Vol. 56, No. 7, pp. 747-771 (2005).

Faraz, Z., ul Haq, S.W., Ali, L., Mahmood, K., Tarar, W.A., Baqai, A.A., Khan, M. and Imran, S.H., "Sheet-metal bend sequence planning subjected to process and material variations," *International Journal of Advanced Manufacturing Technology*, Vol. 88, pp. 815-826 (2017).

Farsi, M.A. and Arezoo, B., "Development of a new method to determine bending sequence in progressive dies," *International Journal of Advanced Manufacturing Technology*, Vol. 43, No. 1, pp. 52-60 (2009).

Gupta, S.K., "Sheet metal bending operation planning: Using virtual node generation to improve search efficiency," *Journal of Manufacturing Systems*, Vol. 18, No. 2, pp. 127-139 (1999).

Kannan, T.R. and Shunmugam, M.S. "Processing of 3D sheet metal components in STEP AP-203 format: feature recognition system," *International Journal of Production Research,* Vol. 47, No. 4, 941-964 (2009-1).

Kannan, T.R. and Shunmugam, M.S. "Processing of 3D sheet metal components in STEP AP-203 format: feature reasoning system," *International Journal of Production Research*, Vol. 47, No. 5, 1287-1308 (2009-2).

Kannan, T.R. and Shunmugam, M.S., "Planner for sheet metal components to obtain optimal bend sequence using a genetic algorithm," *International Journal of Computer Integrated Manufacturing*, Vol. 21, No. 7, pp. 790-802 (2008).

Kim, C., Park, Y.S., Kim, J.H. and Choi, J.C., "A study on the development of computer-aided process planning system for electric product with bending and piercing operations," *Journal of Materials Processing Technology*, Vols. 130-131, pp. 626-631 (2002).

Kim, J.H., Kim, C. and Chang, Y.J., "Development of a process sequence determination technique by fuzzy set theory for an electric product with piercing and bending operation," *International Journal of Advanced Manufacturing Technology*, Vol. 31, No. 5-6, pp. 450-464 (2006).

Kontolatis, N. and Vosniakos, G.-C., "Optimisation of press-brake bending operations in 3D space," *Journal of Intelligent Manufacturing*, Vol. 23, No. 3, pp. 457-469 (2012).

Lin, A.C. and Chen, C.F., "Sequence planning and tool selection for bending processes of 2.5D sheet metals," *Advances in Mechanical Engineering*, Vol. 6, DOI: 10.1155/2014/204930 (2014).

Lin, A.C. and Sheu, D.K., "Knowledge-based sequence planning of shearing operations in progressive dies," *International Journal of Production Research*, Vol. 50, No. 4, pp. 1215-1234 (2012-1).

Lin, A.C. and Sheu, D.K., "Sequence planning for bending operations in progressive dies," *International Journal of Production Research*, Vol. 50, No. 24, pp. 7493-7521 (2012-2).

Márkus, A., Váncza, J. and Kovács, A., "Constraint-based process planning in sheet metal bending," *CIRP Annals*, Vol. 51, No. 1, pp. 425-428 (2002).

Raj Prasanth, D. and Shunmugam, M.S. "Collision detection during planning for sheet metal bending by bounding volume hierarchy approaches," *International Journal of Computer Integrated Manufacturing*, Vol. 31, No. 9, pp. 893-906 (2018).

Rico, C., González, J.M., Mateos, S., Cueata, E. and Valiño, G., "Automatic determination of bending sequences for sheet metal parts with parallel bends," *International Journal of Production Research*, Vol. 41, No. 14, pp. 3273-3299 (2003).

Thanapandi, C.M. Walairacht, A. and Ohara, S., "Genetic algorithm for bending process in sheet metal industry," *Canadian Conference on Electrical and Computer Engineering*, Toronto, ON, Canada, May 13-16, pp. 957-962 (2001).

Thanapandi, C.M., Walairacht, A., Periasamy, T. and Ohara, S., "Preprocessor to improve performance of GA in determining bending process for sheet metal industry," *Proceedings of the 13th International Symposium on Foundations of Intelligent Systems*, Lyon, France, June 27-29, pp. 362-373 (2002).

Tor, S.B., Britton, G.A. and Zhang, W.Y., "A knowledge-based blackboard framework for stamping process planning in progressive die design," *International Journal of Advanced Manufacturing Technology*, Vol. 26, No. 7-8, pp. 774-783 (2005-1).

Tor, S.B., Britton, G.A. and Zhang, W.Y., "Development of an object-oriented blackboard model for stamping process planning in progressive die design," *Journal of Intelligent Manufacturing*, Vol. 16, No. 4, pp. 499-513 (2005-2).

多方向多道次彎曲板金件之電腦輔助折彎順序規劃

林清安
國立臺灣科技大學 機械工程系

陳昭帆
國立臺灣科技大學 自動化及控制研究所

摘 要

在板金打樣的過程中，彎曲加工屬於相當重要的製程，而彎曲加工中折彎順序的規劃則直接影響板金打樣的可行性。因此，本文提出板金件折彎順序規劃的遵循原則，首先從板金件的 3D 幾何模型中搜尋含有最多折彎線的平面，並將此平面設定為折彎基準面，再以折彎基準面上兩條折彎線間最小夾角之原則，將 3D 板金件劃分成多個折彎區域。接著根據折彎操作的幾何特徵，定義六種基本折彎型式，然後將分割後的每一個折彎區域與六種基本折彎型式進行比對，可獲得每個折彎區域的折彎型式組合及折彎順序。最後，採用「最低高度優先處理」的原則進行折彎區域的工作排序，即可獲得整個板金件的折彎順序。